Remote Sensing of Environment 114 (2010) 2146–2159

Contents lists available at ScienceDirect

Remote Sensing of Environment

journal homepage: www.elsevier.com/locate/rse

A Two-Step Filtering approach for detecting maize and soybean phenology with time-series MODIS data

Toshihiro Sakamoto [a,e,*,1], Brian D. Wardlow [a], Anatoly A. Gitelson [b], Shashi B. Verma [c], Andrew E. Suyker [c], Timothy J. Arkebauer [d]

[a] National Drought Mitigation Center, University of Nebraska-Lincoln, Lincoln, Nebraska, USA
[b] Center for Advanced Land Management Information Technologies, University of Nebraska-Lincoln, Lincoln, Nebraska, USA
[c] Great Plains Regional Center for Global Environmental Change, University of Nebraska-Lincoln, Lincoln, Nebraska, USA
[d] Department of Agronomy and Horticulture, University of Nebraska-Lincoln, Lincoln, Nebraska, USA
[e] Ecosystem Informatics Division, National Institute for Agro-Environmental Sciences, Tsukuba, Ibaraki, Japan

ARTICLE INFO

Article history:
Received 17 November 2009
Received in revised form 19 April 2010
Accepted 25 April 2010

Keywords:
Crop phenology
Maize
Soybean
MODIS
Shape-model fitting

ABSTRACT

The crop developmental stage represents essential information for irrigation scheduling/fertilizer management, understanding seasonal ecosystem carbon dioxide (CO_2) exchange, and evaluating crop productivity. In this study, we devised an approach called the Two-Step Filtering (TSF) for detecting the phenological stages of maize and soybean from time-series Wide Dynamic Range Vegetation Index (WDRVI) data derived from Moderate Resolution Imaging Spectroradiometer (MODIS) 250-m observations. The TSF method consists of a Two-Step Filtering scheme that includes: (i) smoothing the temporal WDRVI data with a wavelet-based filter and (ii) deriving the optimum scaling parameters from shape-model fitting procedure. The date of key crop development stages are then estimated by using the optimum scaling parameters and an initial value of the specific phenological date on the shape model, which are preliminary defined in reference to ground-based crop growth stage observations. The shape model is a crop-specific WDRVI curve with typical seasonal features, which were defined by averaging smoothed, multi-year WDRVI profiles from MODIS 250-m data collected over irrigated maize and soybean study sites.

In this study, the TSF method was applied to MODIS-derived WDRVI data over a 6-year period (2003 to 2008) for two irrigated sites and one rainfed site planted to either maize or soybean as part of the Carbon Sequestration Program (CSP) at the University of Nebraska-Lincoln. A comparison of satellite-based retrievals with ground-based crop growth stage observations collected by the CSP over the six growing seasons for these three sites showed that the TSF method can accurately estimate the date of four key phenological stages of maize (V2.5: early vegetative stage, R1: silking stage, R5: dent stage and R6: maturity) and soybean (V1: early vegetative stage, R5: beginning seed, R6: full seed and R7: beginning maturity). The root mean square error (RMSE) of phenological-stage estimation for maize ranged from 2.9 [R1] to 7.0 [R5] days and from 3.2 [R6] to 6.9 [R7] days for soybean, respectively. In addition, the TSF method was also applied for two years (2001 and 2002) over eastern Nebraska to test its ability to characterize the spatio-temporal patterns of these key phenological stages over a larger geographic area. The MODIS-derived crop phenological stage dates agreed well with the statistical crop progress data reported by the United State Department of Agriculture (USDA) National Agricultural Statistics Service (NASS) for eastern Nebraska's three crop agricultural statistic districts (ASDs). At the ASD-level, the RMSE of phenological-stage estimation ranged from 1.6 [R1] to 5.6 [R5] days for maize and from 2.5 [R7] to 5.3 [R5] days for soybean.

1. Introduction

The biophysical characteristics of crops and their physiological response to environment conditions change seasonally with vegetation growth. The phenological stage of a crop represents essential information for irrigation scheduling/fertilizer management, understanding seasonal ecosystem carbon dioxide (CO_2) exchange, and evaluating crop productivity. For maize (*Zea mays*) and soybean (*Glycine max*), which are the target crops in this study, the R1 stage (silking stage) and R4 to R6 stages (full pod to full seed) are quite sensitive to environmental stress in terms of yield reduction (Hickman & Shroyer, 1994; Kilgore & Fjell, 1997).

The majority of maize and soybean in the United States' major production region, the Corn Belt, are cultivated under rainfed conditions and weather conditions are carefully monitored during these critical

* Corresponding author. Ecosystem Informatics Division, National Institute for Agro-Environmental Sciences, Tsukuba, Ibaraki, Japan.
E-mail address: sakamt@affrc.go.jp (T. Sakamoto).
[1] JSPS postdoctoral fellow for research abroad.

0034-4257/$ – see front matter © 2010 Elsevier Inc. All rights reserved.
doi:10.1016/j.rse.2010.04.019

growth stages to estimate year-end crop yields. The timing of a specific phenological stage of maize and soybean can vary from year to year because variations in the start of the planting season, which is highly dependent on soil moisture and temperature conditions, as well as farm-level management decisions (e.g., crop variety and tillage practices). To date, the best available information about the crop developmental stages at a state- to regional-scale have been, Crop Progress Reports (CPRs) published by the United States Department of Agriculture's (USDA) National Agricultural Statistics Service (NASS). CPRs are updated weekly by state NASS offices and report the percentage of a given crop reaching a specific crop development stage (e.g., maize silked or soybean setting pods) over a multi-county agricultural statistic district (ASD) or an entire state (NASS, 2010). ASD-level reports present a general summary of a crop's progress for a number of counties and are insufficient for revealing detailed spatio-temporal patterns in maize and soybean phenology that exist at a relatively local scale across large geographic areas. Field-based, visual surveys of crop phenology are both costly and time consuming, which makes them impractical for large-area crop monitoring activities. Consequently, remote sensing-based techniques offer considerable potential for characterizing regional-scale spatio-temporal patterns and variations in the key phenological stages of maize and soybean. In this context, Moderate Resolution Imaging Spectroradiometer (MODIS) data have become increasingly used for crop mapping and monitoring at a regional scale, because of its unique combination of high temporal (near daily repeat coverage) and moderate spatial (i.e.,250-m and 500-m) resolutions (Brown et al., 2007; Chang et al., 2007; Funk & Budde, 2009; Galford et al., 2008; Ozdogan & Gutman, 2008; Sakamoto, Phung, et al., 2009; Sakamoto et al., 2006; Sakamoto, Van Phung, et al., 2009; Wardlow & Egbert, 2008; Wardlow et al., 2007).

The objective of this paper is to present a Two-Step Filtering (TSF) method, which is a new approach that incorporates the "shape-model fitting" concept, to detect key phenological stages of maize and soybean from the time-series MODIS 250-m WDRVI data. The TSF method was tested over a six-year period (2003 to 2008) for three experimental study sites to assess its robustness to inter-annual climate variations that occur from year-to-year. The performance of this approach was quantitatively validated for estimating several major phenological stages of maize and soybean using near-weekly, ground-based observations of crop growth stages for each site. In addition, we illustrated the advantage of the TSF method by comparing the results to those of two simple alternative approaches that identify the maximum point for detecting the specific phenological stages of maize and soybean from time-series WDRVI data. The TSF method was also applied to time-series MODIS 250 m WDRVI images covering eastern Nebraska for a two-year period (2001 and 2002) to illustrate this approach's capability to characterize regional-scale variations in the targeted maize and soybean phenology stage dates. To validate the regional results, the MODIS-derived phenology date estimates (spatially averaged date across a specific ASD) were compared to crop developmental stage statistics reported by the USDA NASS-CPRs for the two study years.

2. Background and review of remote sensing-based phenology study

Badhwar et al. (1982) proposed a temporal-profile model approach in which parametric curves derived using the exponential and logistic functions were used to classify crop types (e.g., maize, soybean and small grains) from multi-date Landsat greenness data. In addition to crop classification, a series of studies using this temporal-profile model suggested that this type of approach could be used to identify key crop developmental stages for maize (12–14 leaves: V12–14, blister: R2 and full dent: R5), soybean (beginning bloom: R1, beginning seed: R5 and beginning maturity: R7), and spring wheat (jointing, heading and dough) using multi-temporal remote-sensing data (Badhwar, 1984; Bauer, 1985; Henderson & Badhwar, 1982). Then, various satellite-based global imagers such as National Oceanic and Atmospheric Administration's (NOAA) Advanced Very High Resolution Radiometer (AVHRR), National Aeronautics and Space Administration's (NASA), MODIS, and Satellite Pour l'Observation de la Terre (SPOT) VEGETATION, have a temporally-dense time series of near-daily, synoptic observations of the land surface which have been widely used for monitoring seasonal vegetation growth across large geographic areas (Azzali & Menenti, 2000; de Beurs & Henebry, 2004; Jakubauskas et al., 2001, 2002; Kang et al., 2003; Reed et al., 1994; Reed et al., 1996; Xiao et al., 2002). Gallo and Flesch (1989) investigated the usage of NOAA/AVHHR data for monitoring the seasonal growth of maize, and found that the date of maximum normalized difference vegetation index (NDVI) is correspond with the silking stage (R1) for 12 crop-reporting districts in the central United States. Reed et al. (1994) devised 12 seasonal metrics (e.g., onset/end of greenness, time of maximum NDVI and time-integrated NDVI) using the temporal NOAA/AVHRR NDVI data, and suggested that the phenological variability measured from satellite imagery is useful for land cover mapping and phenological interpretation of vegetation's seasonal NDVI dynamics. White et al. (1997) defined the onset/end of greenness when the NDVI ratio exceeds or falls below 0.5 in the smoothed NDVI profile based on the Best Index Slope Extraction (BISE) method (VIOVY et al., 1992) and compared the satellite-based phenology observations of the deciduous broadleaf forest and grassland with the predictions derived from predictive phenology models using meteorological and climatological data.

MODIS 8- and 16-day composite data have been shown to provide sufficient spatial and temporal resolution to detect unique multi-temporal spectral responses from specific crop types for the major crop-producing regions of the United States. Many researchers have demonstrated the utility of time-series MODIS vegetation index (VI) data for classifying specific crop types (Chang et al., 2007; Wardlow & Egbert, 2008; Xavier et al., 2006), discriminating crops under different management practices such as irrigation and multi-cropping (Galford et al., 2008; Ozdogan & Gutman, 2008; Sakamoto et al., 2006; Wardlow & Egbert, 2008; Wardlow et al., 2007; Wardlow et al., 2006), and monitoring general crop phenology (Islam & Bala, 2008; Sakamoto et al., 2005; Wardlow et al., 2006). MODIS' moderate 250-m spatial resolution minimizes the mixed-pixel effect that has limited the application of coarser resolution 1-km data sets from NOAA/AVHRR and SPOT/VEGETATION for detailed crop-related land cover/land use change (LCLUC) characterization (Loveland et al., 1995; Loveland et al., 2000; Townshend & Justice, 1988; Turner et al., 1995). Zhang et al. (2003) applied a series of piecewise logistic functions to 16-day EVI to estimate phenological transition dates (green up onset, maturity onset, senescence onset and dormancy onset) for a mixed forest pixel in New England. Sakamoto et al. (2005) used a wavelet-based filter to smooth 8-day MODIS EVI data and estimated major phenological stages of rice (planting date, heading date and harvesting date) in Japan by detecting characteristic points (maximum, minimum and inflection points) in the smoothed EVI profile. Wardlow et al. (2006) applied the onset date identification method developed by Zhang et al. (2003) to 16-day MODIS 250 m composite NDVI to estimate the green up onset date of summer crops (maize, sorghum, and soybean) across the state of Kansas for 2001. When compared with the NASS-CPR observations, they found the average green up onset differences among the three summer crops to be consistent with relative planting times of maize, sorghum and soybean. They also detected regional, intra-crop date variations due to shifts in the crop calendar because of different growing season lengths. However, their analysis revealed that dense pre-crop vegetation cover (weed/volunteer crop cover) in locations receiving higher amounts of annual precipitation resulted in NDVI values before planting, which led to misidentification of the green up onset (i.e., early bias) for those areas.

The similarity among the previous studies highlighted above is that specific phenological dates of natural vegetation and crops were

estimated by detecting preliminary-defined metrics (e.g. fixed-threshold value, seasonal midpoint, maximum point and inflection point) from the time-series VI data. However, if the VI observations near the local temporal period of an expected event include a noise component, the temporal position detected by these specific metrics can be dramatically shifted (e.g., much earlier or later than an expected date range), depending on these subtle non-vegetation-related changes in the temporal VI profile. Therefore, commonly used phenology detection methods using specific metrics are sensitive to observation errors and noise caused by atmospheric constituents (e.g., water vapor), thick cloud coverage, bi-directional reflectance distribution function (BRDF) effect, and the mixed-pixel effect due to viewing geometry in the MODIS data products. As a result, considerable phenological date estimate errors can be introduced when these traditional methods are applied to time-series data with these types of noise components. Therefore, improved crop phenology detection methods are needed that are robust against the subtle non-vegetation-related VI fluctuations (e.g., residual sub-pixel cloud cover) that may remain in the atmospherically-corrected, standard MODIS 250 m VI data.

Another challenge in remote sensing phenology studies has been the quantitative validation of phenological data estimates, which is critical for understanding the applicability of this information. Despite crops having well-defined crop calendars, such validation exercises have been extremely limited (Sakamoto et al., 2005; Wardlow et al., 2006), primarily because ground-based, field-level observations about the timing of specific agronomic growth stages is lacking. Both Sakamoto et al. (2005) and Wardlow et al. (2006) used district-level statistical crop progress data as a general approximation of phenology status over relatively large geographic areas to validate MODIS-based crop phenology date estimates. However, the crop progress data lacked the spatial precision to thoroughly assess the accuracy field-level estimates, as well as local-scale variations in the dates of a specific phenological stage that occur across these multi-county USDA reporting districts, and more precise validation of the remote-sensing based estimates using ground-based crop growth stage observations is required.

3. Study sites and ground-based observation data

The ground-based crop growth stage observations were obtained at three study sites, maintained as part of the Carbon Sequestration Program (CSP) at the University of Nebraska-Lincoln's (UNL) Agricultural Research and Development Center (http://csp.unl.edu/Public/sites.htm) in eastern Nebraska (Fig. 1). Study sites 1 (41°9′54.2″N, 96°28′.9″W) and 2 (41°9′53.5″N, 96°28′12.3″W) are approximately 40 ha and irrigated by a center-pivot irrigation system. Site 3 (41°10′46.8″N, 96°26′22.7″W) is a rainfed site that is approximately 60 ha. Site 1 has been continuously planted to maize since 2001, while sites 2 and 3 have been planted in a maize (odd years)–soybean (even years) rotation (Table 1). In this paper, these three study sites will be referenced according to their respective cultivation methods as the Irrigated Continuous Maize (ICM) for Site 1, Irrigated Maize–Soybean (IMS) for Site 2, and Rainfed Maize–Soybean (RMS for Site 3). In general, maize is planted earlier (late-April to early-May) than soybean (mid- to late-May), but the actual planting dates of both crops can slightly vary from year to year (Table 1) depending on weather and soil moisture conditions.

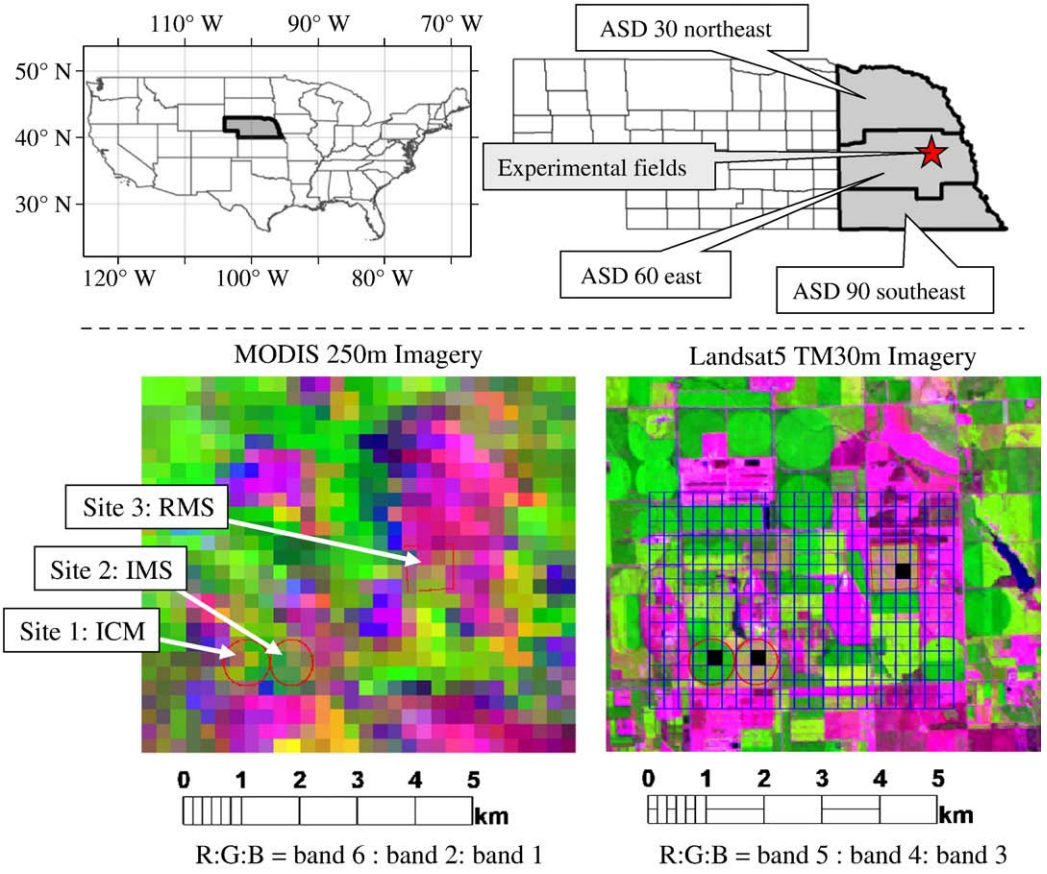

Fig. 1. The location of the study sites in Nebraska, and a comparison between MODIS and Landsat5 TM false color images over the same region. The blue grid lines over Landsat5 TM image show the pixel spacing of MODIS 250 m imagery, and three black-filled grids on each experimental site indicate the MODIS-sampling pixels. The MODIS 250 m image was acquired on July 12–19, 2006, and the band 6 data is derived from the spatially interpolated MODIS 500 m imagery. The Landsat5 TM image was acquired on July 18, 2006.

Table 1
The cultivated crops and planting date (DOY) in each year.

Year	Site 1: ICM	Site 2: IMS	Site 3: RMS
2001	Maize (130)[a]	Maize (131)	Maize (134)
2002	Maize (129)[a]	Soybean (140)[b]	Soybean (140)
2003	Maize (135)[a,c]	Maize (134)[c]	Maize (133)[c]
2004	Maize (126)[a,c]	Soybean (154)[b,c]	Soybean (155)[c]
2005	Maize (124)[a,c]	Maize (123)[c]	Maize (117)[c]
2006	Maize (125)[a,c]	Soybean (132)[c]	Soybean (131)[c]
2007	Maize (121)[a,c]	Maize (122)[c]	Maize (122)[c]
2008	Maize (120)[a,c]	Soybean (136)[b,c]	Soybean (135)[c]

[a] The data used for making the shape model of maize.
[b] The data used for making the shape model of soybean.
[c] The ground-observed phenology data were compared with the MODIS-derived estimations.

The targeted phenological stages of maize and soybean and a description of each stage's plant physiological features are listed in Table 2 (Hickman & Shroyer, 1994; Kilgore & Fjell, 1997). The dates of these phenological stages are essential information for projecting potential crop yield and assessing percentage sterility under abnormal weather conditions. The ground-based crop growth stage observations were conducted by agronomists as part of the CSP once every 3–10 days during the 2003 to 2008 growing seasons (note: the time of occurrence of maize-R6 stage on IMS in 2003 was not recorded). The total number of comparative samples used for validation (i.e., sum of the total number of years each of the sites was planted with a specific crop) was 47 for maize and 24 for soybean. Because the growth rate may vary by a few days between individual plants in a site, it is difficult to determine the exact date when an entire crop completes the transition from one phenological stage to the next unless ground-based observation is conducted every day. Although the ground-based observations may have a slight margin of error of a few days caused by the longer temporal interval between visual agronomic assessments, the sites are assumed to represent a relatively homogeneous phenological state when compared to the 250 m-pixel footprint being analyzed in this study.

4. MODIS WDRVI data

This study used an 8-day time series of 250 m and 500 m MODIS surface reflectance data (MOD09Q1 and MOD09A1, Collection 5, tile: h10v04), acquired from 2001 to 2008. The specific data layers used in the WDRVI calculations were the 250 m red (Band 1) and near infrared (NIR) reflectance (Band 2) data from the MOD09Q1 product and the 500 m blue reflectance (Band 3) and the observation date (DOY) from the MOD09A1 product. The map projection was converted from Sinusoidal to Universal Transverse Mercator (UTM, Zone 14 and WGS-84) using ENVI (ITT Visual Information Solutions) image-processing software. The blue reflectance and the observation date bands, which are required for cloud-cover detection in the time series data processing, were resampled from 500 m to 250 m resolution using the nearest-neighbor method. In Fig. 1, the blue grid lines overlaid on the Landsat TM 30 m imagery represent the corresponding MODIS 250 m pixel footprint locations over the three study sites. The actual ground area sampled for each MODIS pixel can vary depending on the sensor view angle on the date at which that location is observed in the 8-day composite image. Therefore, it is inevitable that the surrounding land cover types can affect the spectral response of the target MODIS pixel with the greatest affects occurring for off-nadir observations.

The WDRVI has a higher sensitivity to changes at moderate to high biomass than the NDVI and has been found to have a linear relationship with the green leaf area index (LAI) of both maize and soybean (Gitelson, 2004; Gitelson et al., 2007). Therefore, the WDRVI was selected for this study because it was shown to be able to track subtle changes in LAI of both crops during their moderate to high biomass growth stages. WDRVI is calculated by the following equation:

$$WDRVI = (\alpha\rho_{NIR} - \rho_{red}) / (\alpha\rho_{NIR} + \rho_{red}) \quad (1)$$

where ρ_{NIR} and ρ_{red} are the MODIS surface reflectance values in the NIR band (841–875 nm, Band 2) and the red band (621–670 nm, Band1) and α is a weighting coefficient. According to Gitelson et al. (2007), the optimum value of α is 0.2 for linearly-quantifying the green LAI of maize and soybean, which was used to calculate the MODIS WDRVI.

5. Methodology: Two-Step Filtering (TSF) method for detecting crop phenological stages

A simplified schematic of the TSF methodology is shown in Fig. 2. The TSF method consists of Two-Step Filtering procedure that includes smoothing the temporal WDRVI data with a wavelet-based filter and then deriving the optimum scaling parameters that fit the shape model on the smoothed WDRVI data. A one-step estimation procedure was then used to estimate the phenological date from the optimum scaling parameters and the preliminary defined phenological date on the shape model (x_0; Fig. 2, Table 2 and Eq. (3)).

In the initial step, a wavelet-based filter was used to reduce the high-frequency noise component (e.g., cloud cover and mixed-pixel effect caused by larger view angles) in the temporal WDRVI data. This filtering technique applied to time-series VI data has been utilized for monitoring crop phenology, regional flood expansion, and farming systems (Galford et al., 2008; Sakamoto et al., 2007; Sakamoto, Van, et al., 2009). The shape model is the crop-specific WDRVI curve that represents the typical seasonal WDRVI response of the crop, which was generated by averaging the multi-year smoothed WDRVI profiles for both maize and soybean from the CSP irrigated study sites. Because of targeted water applications on both irrigated sites to reduce water stress, the inter-annual variation in WDRVI profiles of the irrigated sites is assumed to be less than that on the rainfed sites and represent an idealized multi-temporal VI response of the crop. As a result, we assumed that the shape model is linearly scalable to fit the time-series VI profile of either crop's growth pattern by geometrical scaling, which can vary from year to year due to weather conditions and is dependent on a field's location and management type.

The optimum scaling parameters for fitting the preliminary defined shape model on each smoothed time series of WDRVI data

Table 2
Target phenological stages in time-series analysis.

Stage		State title	x_0[a] [DOY]	Description
Maize	V2.5	Vegetative stage	150	Second or third leaf is fully expanded
	R1	Silking stage	200	Silk is grown out from top of bract leaf after tassel emergence. This stage is most sensitive to drought stress.
	R5	Dent stage	240	Kernels are drying and denting. The color of shelled cob is dark red.
	R6	Maturity	265	All kernel on ear attain maximum dry weight.
Soybean	V1	Vegetative stage	170	Leaves at unifoliate nodes are fully developed
	R5	Beginning seed	225	Seeds in pod are filled by using large amounts of water and nutrients. R4–6 stages are most sensitive to environmental stress
	R6	Full seed	240	Color of bean is still green. Total pod weight will peak.
	R7	Beginning maturity	270	Dry matters attains on peak.

[a] x_0 is the preliminary-defined phenological date on the shape model references related the description: Hickman and Shroyer (1994) and Kilgore and Fjell (1997).

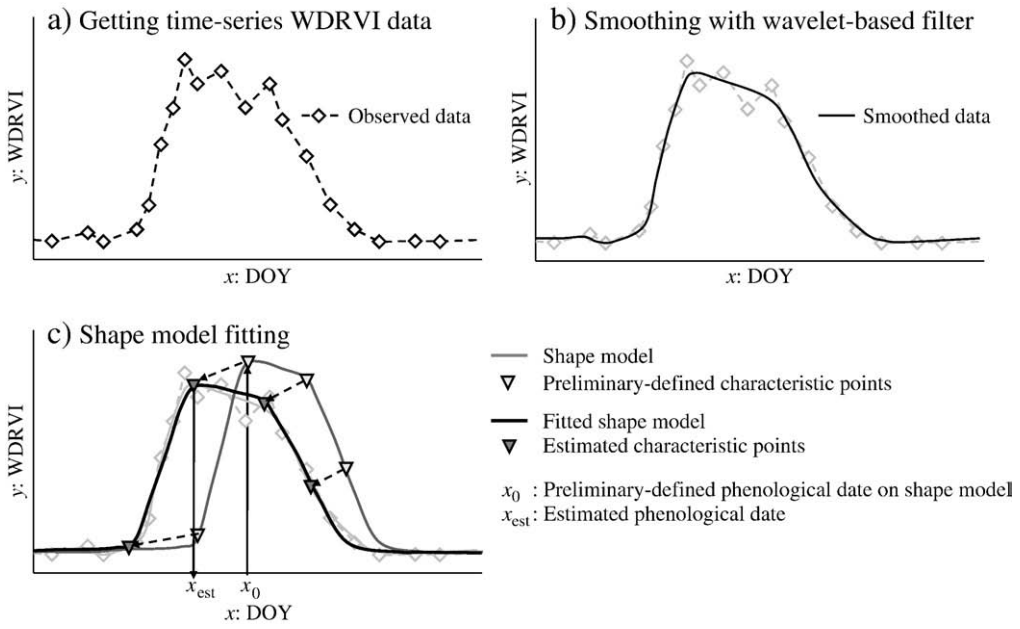

Fig. 2. Simplified schematic presenting the procedure of the Two-Step Filtering method.

are sought by optimization analysis based on Generalized Reduced Gradient Code (Lasdon et al., 1978). Finally, the timing estimation of the objective phenological stages is derived from the geometric equation (Eq. (3) described later) coupled with the preliminary defined phenological dates on shape model (x_0; Fig. 2, Table 2 and Eq. (3)) and the optimum scaling parameters.

5.1. Wavelet-based filter for smoothing MODIS WDRVI data

The MODIS surface reflectance data (MOD09 product) were corrected for the effects of gaseous absorption, molecules and aerosol scattering (Vermote et al., 2002). In the 8-day composite product, the spatial extent of cloud coverage and the inclusion of extreme off-nadir observations are minimized through an 8-day constrained view maximum value compositing technique. In spite of the rigorous, systematic atmospheric corrections applied to the MODIS spectral data, the observed WDRVI time-series data still contain short-term fluctuations (i.e., between consecutive 8-day periods) with many abnormally high values (i.e., spikes) that are unrelated to seasonal changes in vegetation conditions (Fig. 2). As discussed earlier, a noise component often remains in time-series remote sensing data such as the standard MOD09 products for various reasons, including persistent cloud cover, BRDF effects, and mixed-pixel effects caused by the moderate spatial resolution of the sensor, particularly for observations acquired at higher view angles. Therefore, it is necessary to reduce the noise components from the observed time-series WDRVI data to minimize their influence on the phenological date estimates. The observed, multi-temporal WDRVI profile was smoothed with a wavelet-based filter to minimize this remaining noise artifact in the time series observations as the first step in the TSF approach.

In correcting the time-series MODIS data, any pixel with a reflectance value greater than 0.2 in the blue band was defined as a cloud-covered pixel and was treated as a missing observation in the temporal sequence of WDRVI data. Linear interpolation between the periods with valid WDRVI was used to assign values to the periods with these missing observations. The WDRVI data in reference to the observation date reported in the date band of the MOD09 product were then temporally resampled at equally spaced 5-day intervals. The components with a frequency higher than a scale of 4 in the 5-day interval input array (<80 days $=2^4\times5$) were removed through wavelet transformation and wavelet inverse transformation using a specific mother wavelet (coiflet, order $=4$) in order to reduce the high-frequency noise components probably related to uncorrected atmosphere effect or mixed-pixel effect caused by the variable view angle. See Sakamoto et al. (2005) for details about the wavelet-based filter.

5.2. Making a shape model

The shape models used in this study, which represent the typical multi-temporal trajectory of a WDRVI profile for each crop, are not expressed by a mathematical formulation like the approaches used by Badhwar (1984) and Zhang et al. (2003) that smoothed the temporal VI data with parametric curves defined by exponential and logistic function and double logistic functions, respectively. The shape models for maize and soybean were defined by averaging the multi-year smoothed WDRVI data acquired on the two irrigated study sites (Fig. 3). In order to make the discriminative crop-specific WDRVI curves, the smoothed WDRVI data of the ICM site for eight years (2001–2008) were used for the maize shape model, and data from the IMS site for three years (2002, 2004 and 2008) were used to create the soybean shape model. The data of IMS 2006 was excluded from the input data for making the soybean shape model because an unexpected feature (bi-modal peak) during the middle of the growing season appeared in the time series that year, which was unrepresentative of the soybean's multi-temporal WDVRI behavior. The time-series WDVRI data from the center pixel of each irrigated site was used to develop the shape model for each crop rather than using all pixels over the site in order to minimize the influence of mixed pixel responses in the develop of these idealized WDRVI curves. A total of 8 WDRVI annual time series were used to develop the maize shape model and 3 WDRVI time series to create the soybean shape model. The pixel locations used for making the shape model were the same as where the site observations were carried out. The temporal features of the shape models derived for maize and soybean presented in Fig. 3 were found to be quite similar to the ground-measured LAI data collected across the growing season on the corresponding study sites (Suyker & Verma, 2009).

5.3. Fitting the shape model on the smoothed WDRVI data

The optimum scaling parameters (*xscale*, *yscale*, and *tshift*) that approximate the fit of the shape model to the smoothed WDRVI data

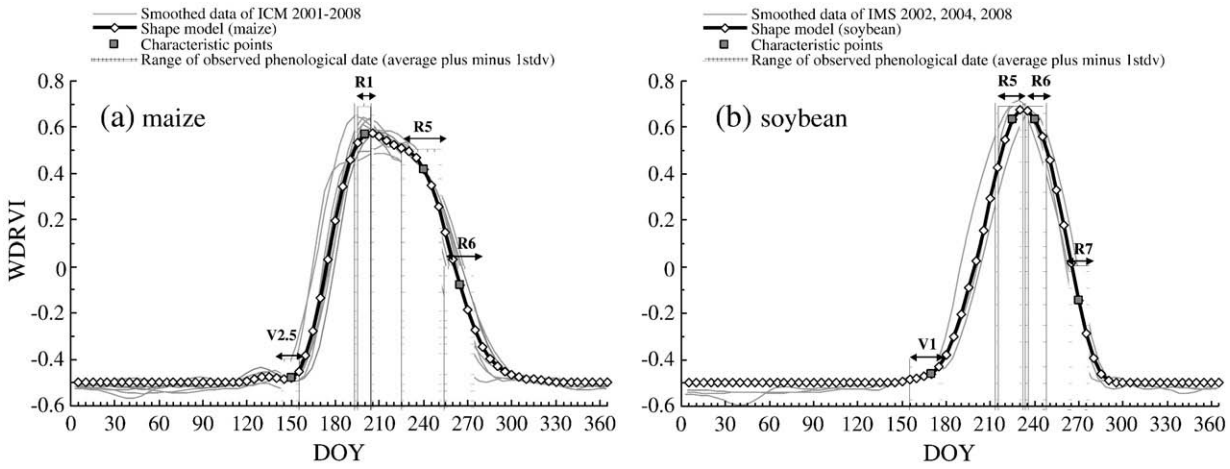

Fig. 3. Preliminary definition of the shape model and characteristic points indicating the specific phenological stages of (a) corn and (b) soybean.

were automatically calculated based on the smallest root mean square error (RMSE) between the scaled shape model and the smoothed WDRVI data (Eq. (2)) by an IDL program (ITT Visual Information Solution) using a subroutine named "CONSTRAINED_MIN", which provides optimization analysis based on Generalized Reduced Gradient Code (Lasdon et al., 1978). The search ranges for each parameter were empirically determined as follows: $0.3<xscale<1.5$, $0.3<scale<1.5$ and $-80<tshift<80$.

$$RMSE = \left[\frac{1}{73}\sum_{x=5,10,15,\ldots}^{365}(f(x)-g(x))^2\right]^{\frac{1}{2}} \quad (2)$$

The function $f(x)$ implies the smoothed WDRVI data for a given site or year, where x is the day of year (DOY). In the scaled shape model, $g(x)$ is transformed from the shape model $h(x)$ as follows:

$$g(x) = yscale \times h(xscale \times (x_0 + tshift) + 0.5) - 0.5 \quad (3)$$

where *xscale*, *yscale* and *tshift* are scaling parameters. The x_0 term is a preliminary-defined phenological date on the shape model (Fig. 2, Table 2).

The WDRVI value in the agricultural off-season occasionally falls below −0.5 for many days because of snow cover and bare ground during the winter months. The WDRVI values (typically < −0.5) for dates outside the agricultural growing season periods (empirically defined as DOY: 1–100 and 320–365) were replaced with a constant WDRVI lower limit value (−0.5) in both the smoothed WDRVI data and the shape model. This process was also intended to eliminate the effects of snow cover and weed coverage before crop growing season.

The summary of the optimum scaling parameters is presented in Table 3. The *yscale* represents the relative magnitude of green LAI throughout the entire growing season based on the shape model. The mean values of *yscale* at the RMS site were relatively lower than those at the ICM and IMS sites. In addition, the standard deviation of *yscale* at the RMS site was higher than those at the ICM and IMS sites. According to the ground-based LAI observation (Suyker & Verma, 2009), the maximum LAI at the RMS site tended to be lower than that at the ICM or IMS site from 2001 to 2005. Given that the vegetation growth at the RMS site is inhibited by drought stress and lower planting density, it can be said that the difference in the inter-annual changes of vegetation activity between the irrigated sites (ICM and IMS) and the rainfed site (RMS) is reflected in the statistical value of the *yscale* parameter.

Both *xscale* and *tshift* are related to time dimension (Eq. (3)). The standard deviations of *xscale* and *tshift* at the RMS site were also higher than at the ICM or IMS site. The difference in the crop growing duration (V2.5–R6 for maize and V1–R7 for soybean) between the irrigated sites (ICM and IMS) and the rainfed site (RMS) is shown in Table 4. The growing duration at the RMS site tended to be shorter with a higher standard deviation than at either irrigated site. Thus, it can be said that the combination of both parameters represents the difference in the inter-annual changes of the growing season conditions and duration.

5.4. Estimating phenological date using optimum scaling parameters

The significance of the target phenological stages of maize and soybean are summarized in Table 2. The response of crop yield to environmental stress varies depending on the crop developmental stage. It is noted that drought stress around maize R1 stage can easily reduce final yield of maize by 30% (Hickman & Shroyer, 1994), and various environmental stress (moisture, high temperature and hail)

Table 3
Summary of the optimum scaling parameters for 6 years (2003–2008).

Crop	Management	*xscale*				*yscale*				*tshift*				*n*[a]
		Mean	Max	Min	Stdev	Mean	Max	Min	Stdev	Mean	Max	Min	Stdev	
Maize	ICM	0.98	1.08	0.90	0.06	1.01	1.06	0.96	0.04	3	26	−13	14	6[b]
	IMS	1.01	1.03	0.97	0.04	0.96	0.98	0.92	0.04	−3	5	−12	8	3
	RMS	0.94	1.07	0.82	0.13	0.88	0.95	0.83	0.07	11	40	−17	29	3
Soybean	IMS	1.01	1.10	0.95	0.08	0.99	0.99	0.98	0.01	−2	12	−25	21	3[c]
	RMS	1.00	1.11	0.87	0.12	0.98	1.05	0.93	0.06	−1	31	−27	30	3

[a] *n* is number of the comparison data.
[b] Includes the 6 pixels used for making the shape model (ICM 2003–2008).
[c] Includes the 2 pixels used for making the shape model (IMS 2004, 2008).

Table 4
The difference in the observed growing season length of maize and soybean between the irrigated sites and the rainfed site for 6 years (2003–2008).

Crop	Management	Growing duration (V2.5–R6 for maize, V1–R7 for soybeans)				
		Mean	Max	Min	Stdev	n[a]
Maize	ICM	115.7	129.0	110.0	6.8	6
	IMS	115.0	119.0	111.0	5.7	2
	ICM + IMS	115.5	129.0	110.0	6.2	8
	RMS	106.0	116.0	91.0	13.2	3
Soybean	IMS	104.3	110.0	96.0	7.4	3
	RMS	101.3	108.0	91.0	9.1	3

[a] n is number of observations.

especially from soybean R4.5 through R5.5 stage reduce final yield of soybean (Kilgore & Fjell, 1997).

Fig. 3 shows the multi-year smoothed WDRVI data used to define the maize and soybean shape models and the temporal windows for each targeted phenological stage, which represent the average date ±1 standard deviation of the dates across the multiple years of ground observations. The default constants that indicate the relative temporal positions of these phenological stages in both shape models (i.e., the preliminary defined phenological dates on the shape model: x_0) are empirically defined in reference to these temporal windows for each phenological stage and the curve line features of the shape models. The preliminary defined phenological dates (x_0) on the shape models (Fig. 3) are listed on Table 2.

In Fig. 3, both the maize V2.5 stage and soybean V1 stage occur just before a rapid increase of WDRVI during which both crops experience a rapid green up as their vegetated canopies develop. The maize R1 stage and the soybean R5 stage occur near the point of the maximum WDRVI values on each shape model. The preliminary defined position of maize R1 stage near the time of the maximum WDRVI value is consistent the timing of the silking stage (R1) that normally occurs within 2 or 3 days of maize's maximum green leaf area (Dale et al., 1980; Gallo & Flesch, 1989). The maize R5 stage occurs near the start of senescence, which is marked by a decrease of WDRVI values on the shape model as leaves begin to desiccate and chlorophyll content declines. Soybean R6 stage occurs just after the WDRVI maximum point. Distinctive points like local maximum and inflection points were not observed on the shape models near the maize R6 and soybean R7 stages when both crops reach near their maturity or begging mature stage. The timing of this maturity occurs in the middle of the senescence phase, which corresponds to approximately the mid-point in the decline of WDRVI values between DOY 240 and 295 on both crops' shape models, respectively.

The remote sensing-based phenological date is estimated from the optimum scaling parameters and the preliminary determined phenological date (Table 2). The formula is as follows:

$$X_{est} = xscale \times (x_0 + tshift) \quad (4)$$

where X_{est} is an estimated phenological date, x_0 is a default constant that is the same as the preliminary defined phenological date (Table 2), and *xscale* and *tshift* are the optimum scaling parameters derived in the shape model fitting.

6. Simple methods of phenological date estimation without shape model fitting

In terms of the algorithm used in the TSF method to detect the key phenological stages, the methodological approach is quite different from that of conventional methods that use specific metrics defined by the local variations in the multi-temporal VI data. To illustrate the advantage of the TSF method, it was compared to two alternative methods that rely on the identification of the maximum VI, which is one of the more commonly used metrics to detect the specific timing related to the seasonal vegetation growth stages from time-series VI data (Galford et al., 2008; Gallo & Flesch, 1989; Hill & Donald, 2003; Islam & Bala, 2008; Reed et al., 1994; Sakamoto et al., 2005). The first method detects the maximum point from the original, unsmoothed WDRVI data (referred to as the ORG method). The second method detects the maximum point from the smoothed WDRVI data derived from the wavelet-based filter (referred to as the WDF method). These methods do not rely on a complicated algorithm to identify the maximum point; thus the two methods are collectively referred to as 'simple' methods in this paper. Fig. 4 shows the data-flow diagram of the TSF method and the two alternative methods (ORG and WBF), which estimate dates of the maize R1 and the soybean R5 stages.

The point at which the green vegetation fraction (i.e., the peak WDRVI value) changes from an increasing to a decreasing mode is expected to be coincident with bio-physiological changes related to crop phenology. For example, the maximum point of the time-series EVI data is coincident with the rice-heading season (Sakamoto et al., 2005). We chose the maize R1 and the soybean R5 as the target phenological stages to compare the TSF to the two simple methods because these phenological events occur near the peak in the time-series WDRVI data (Fig. 3). According to the preliminary comparison with the phenological date of the ground-based observations from 2003 to 2008 at the CSP experimental sites (Fig. 1), we found that both phenological stages occur a few days before the WDRVI maximum point. On the basis of these observations, the ORG and WBF methods

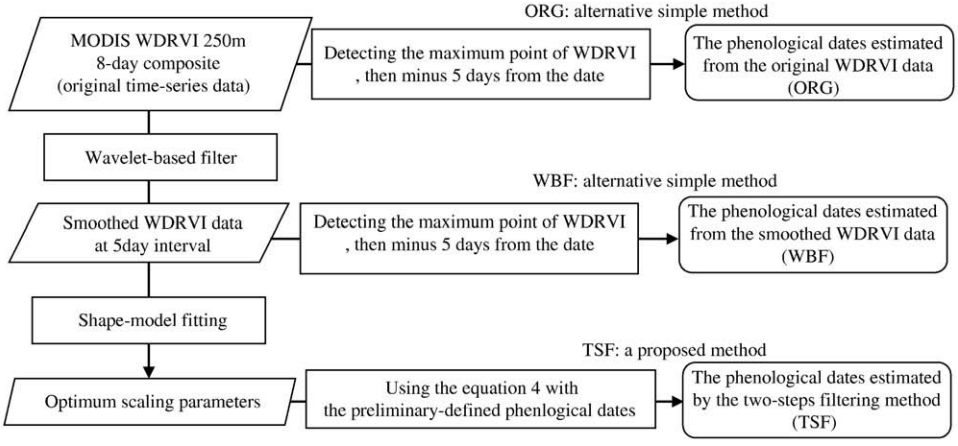

Fig. 4. Data-flow diagram of the Two-Step Filtering method (TSF) and two alternative simple methods (named as ORG and WBF) for estimating phenological dates, R1 of maize and R5 of soybean.

estimates the maize R1 and soybean R5 dates by identifying 5 days prior date of the maximum WDRVI point from the original time-series WDRVI data (ORG) and the smoothed time-series WDRVI data (WBF), respectively.

7. Region-based verification: detecting spatial distribution of the phenological dates of maize and soybean in the eastern Nebraska

7.1. Cropland Data Layers (CDL)

In this study, we used NASS Cropland Data Layers (NASS-CDL) for Nebraska in 2001 and 2002 to select target maize and soybean pixels over three ASDs (ASD 30 — northeast, ASD 60 — east, and ASD 90 — southeast) in eastern Nebraska (Fig. 1) to test the performance of the TSF method over a larger geographic area. The regional assessment was limited to just three ASDs because the NASS-CDL only covered a limited area of the state (Landsat path 26, rows 31 and 32) for 2001 that comparable ASD-level crop progress data were available (discussed in next section). The NASS-CDL classifies specific crop types and is generated using Landsat 5 Thematic Mapper (TM) and Landsat 7 Enhanced Thematic Mapper (ETM+) data (http://www.nass.usda.gov/research/Cropland/SARS1a.htm). The original 30-m NASS-CDL data was resampled using the nearest neighbor approach to a 25-m grid to allow for easy calculation of the total area occupied by maize and soybean within each 250-m MODIS pixel footprint. An area-ratio threshold of 75% (i.e., >75% of a 250 m pixel's area was occupied by maize or soybean) was adopted to select the specific MODIS 250 m pixels across the region to apply the TSF method. A relatively high area-ratio threshold (75%) was empirically determined to reduce the number of mixed pixels containing large percentages of multiple land cover types entering into the analysis with the goal of collecting a representative geographic sample of both crops across the three districts. A total of 302,113 and 274,648 pixels were selected for maize and soybean, respectively.

7.2. Crop Progress Reports (CPR)

Weekly crop progress information about maize and soybean reported by the Nebraska Agricultural Statistics Service (NASS, 2010) was used as the reference data set maize to evaluate the accuracy of MODIS-derived, phenological estimates for the three ASDs. These progress reports of crop developmental stages are recorded as area ratio at the ASD-level in Nebraska for a limited number of years including 2001 and 2002. The Nebraska Agricultural Statistics Service stopped producing ASD-level information of crop growing condition after 2002 limiting the study period of the regional evaluation. For this analysis, the weekly area ratio of each crop developmental stage was linearly interpolated to calculate the median date at which the interpolated area ratio based on the NASS-CPRs reached 50%. The median crop phenological dates of the NASS-CPR were compared to with the MODIS-derived estimates, which were calculated as the median dates across all selected maize and soybean pixels across each ASD.

The crop developmental stages recorded in NASS-CPR are not completely same as those defined in the MODIS-derived estimations. Therefore, the general crop development stages in the NASS-CPRs were matched with a specific agronomic stage estimated form WDRVI data based on their similar timing in maize and soybean's growth cycles. For maize, four NASS-CPR/MODIS-derived crop stage pairs were used for comparative purposes, which include: Maize Emerged vs. MODIS V2.5, Maize Silked vs. MODIS R1, Maize Dent vs. MODIS R5, and Maize Maturity vs. MODIS R6. For soybean, three NASS CPR/MODIS-estimated crop development stages were paired, which included: Soybean Emerged vs. MODIS V1, Soybean Setting Pods vs. MODIS R5, and Soybean Dropping Leaves vs. MODIS R7.

8. Results and discussion

8.1. Pixel-based verification with ground-based observation data

The management-specific results of the TSF method for estimating four specific phenological stages of maize and soybean are presented in Tables 5 and 6, and a comparison between the MODIS-derived estimates and the ground-based crop growth observations are shown in Fig. 5. The phenological stages with the highest estimation accuracy were the R1 stage for maize (RMSE: 2.4 days, correlation coefficient: $R=0.84$) and the R6 stage for soybean (RMSE: 3.0 days, $R=0.87$), both of which occur at or near the maximum WDRVI point in the preliminary defined shape model (Fig. 3). Maize and soybean are similar to rice in the sense that their most sensitive phenological stage to environmental stress, which can result in yield reductions, occurs around the peak point of the temporal VI profile when the green LAI is near its maximum. As with the heading stage of rice (Sakamoto et al., 2005), the transition stage that follows the seasonal VI peak in maize coincides with tasseling and the initial decline in green leaf area due to the senescence during the reproductive stages. Because this seasonal VI peak marks the point at which the VI values decrease after reaching peak greenness, the alteration in the shape of the local VI profile around the maximum point is clearer than the other phenological stages such as green up or senescence, which occur around inflection points.

As for the other phenological stages of maize and soybean, the RMSE of the estimated dates versus the ground-based crop growth stage observations were less than 9 days for all crop/management combinations. Overall, the performance for estimating the other three

Table 5
Accuracy assessment of the estimated phenological date and period against the ground-observation data by using root mean square error (RMSE) and correlation coefficient (R) for maize.

Stage/period	Management	RMSE (days)	R	n[a]
V2.5	ICM	3.5	0.81	6[b]
	IMS	3.2	–	3
	RMS	4.6	–	3
	IMS + RMS	4.0	0.82	6
	ICM + IMS + RMS	3.7	0.79	12[b]
R1	ICM	0.7	0.99	6[b]
	IMS	2.4	–	3
	RMS	4.1	–	3
	IMS + RMS	3.4	0.59	6
	ICM + IMS + RMS	2.4	0.84	12[b]
R5	ICM	8.6	0.74	6[b]
	IMS	6.9	–	3
	RMS	4.9	–	3
	IMS + RMS	6.0	0.48	6
	ICM + IMS + RMS	7.4	0.61	12[b]
R6	ICM	4.0	0.90	6[b]
	IMS	3.5	–	2
	RMS	4.7	–	3
	IMS + RMS	4.3	0.97	5
	ICM + IMS + RMS	4.1	0.90	11[b]
V2.5–R1	ICM	3.4	0.18	6[b]
	IMS	3.1	–	3
	RMS	4.1	–	3
	IMS + RMS	3.7	0.64	6
	ICM + IMS + RMS	3.5	0.52	12[b]
R1–R6	ICM	3.9	0.74	6[b]
	IMS	2.2	–	2
	RMS	7.4	–	3
	IMS + RMS	5.9	0.84	5
	ICM + IMS + RMS	4.9	0.77	11[b]
V2.5–R6	ICM	4.9	0.73	6[b]
	IMS	1.1	–	2
	RMS	5.7	–	3
	IMS + RMS	4.5	0.93	5
	ICM + IMS + RMS	4.7	0.85	11[b]

[a] n is number of the comparison data.
[b] Includes the 6 pixels used for making the shape model (ICM 2003–2008).

Table 6
Accuracy assessment of the estimated phenological date and period against the ground-observation data by using root mean square error (RMSE) and correlation coefficient (R) for soybean.

Stage/period	Management	RMSE (days)	R	n[a]
V1	IMS	5.1	–	3[b]
	RMS	7.8	–	3
	IMS + RMS	6.6	0.66	6[b]
R5	IMS	4.2	–	3[b]
	RMS	5.8	–	3
	IMS + RMS	5.1	0.68	6[b]
R6	IMS	2.2	–	3[b]
	RMS	3.7	–	3
	IMS + RMS	3.0	0.87	6[b]
R7	IMS	5.4	–	3[b]
	RMS	8.3	–	3
	IMS + RMS	7.0	−0.13	6[b]
V1–R5	IMS	1.9	–	3[b]
	RMS	7.9	–	3
	IMS + RMS	5.7	0.00	6[b]
R5–R7	IMS	7.1	–	3[b]
	RMS	9.6	–	3
	IMS + RMS	8.5	−0.17	6[b]
V1–R7	IMS	8.7	–	3[b]
	RMS	14.5	–	3
	IMS + RMS	11.9	−0.17	6[b]

[a] n is number of the comparison data.
[b] Includes the 2 pixels used for making the shape model (IMS 2004, 2008).

targeted growing season periods was also good for maize (RMSE ranged from 0.7 to 7.4 days; Table 5), but the error was slightly higher for soybean (RMSE ranged from a difference of 1.9 to 14.5 days; Table 6). There was no consistent trend (later or earlier) in the differences between the estimated and the observed dates for both maize and soybean (Fig. 5c and d). The performance of the TSF in estimating soybean's V1 and R7 stages (Table 6) was not as good as it was for the other phenological stages/periods with 5–7 days differences between the estimated and observed dates of these specific stages. In addition, the largest differences of estimation accuracy were found for these two soybean stages between the IMS and RMS sites. As a result, a lower estimation accuracy for growing season length was attained for soybean (RMSE for V1–R7: 11.9 days) as compared to maize (RMSE for V2.5–R6: 4.7 days). Comparing the temporal period defining the growing season when both crops were actively growing based on the WDRVI data of the shape models (i.e., periods of WDRVI>-0.3), the period length for maize was 20 days longer than that of soybean. In Fig. 3, this longer period length for maize is exhibited by a wider uni-modal WDRVI peak than soybean. The shorter period length of soybean (DOY: 185–275, length: 90 days) results in fewer time-series MODIS observations being used to generate the growing season length WDRVI profile, which can result in a greater alteration of the profile's multi-temporal behavior if a bad/poor quality observation, is encountered as compared to the longer period length of maize (DOY: 165–275, length: 110 days). As a result, the shape of the soybean WDRVI profile is more susceptible to changes in the data quality of the time-series observations, which may have resulted in the slight higher date errors. Further work is needed to fully understand the influence of data quality on multi-temporal VI profiles and phenology date calculation, which was beyond the scope of this research. Another consideration for the reduced performance of the TSF method for soybean is the smaller sample size ($n=3$) used to define the soybean shape model compared to maize ($n=8$). Increasing the number of sampled pixels for soybean may have resulted in a more representative shape model and improved the estimation accuracy of the TSF method for this crop.

According to the ground-based green LAI measurements for maize from 2001 to 2005 (Suyker and Verma, 2009), the senescence of maize in 2003 at the RMS site was earlier and the temporal window for the LAI decline to zero was shorter than in the other years of the study period. The shorter growing season length of maize in 2003 on this rainfed site (RMS site) was likely the result of severe drought

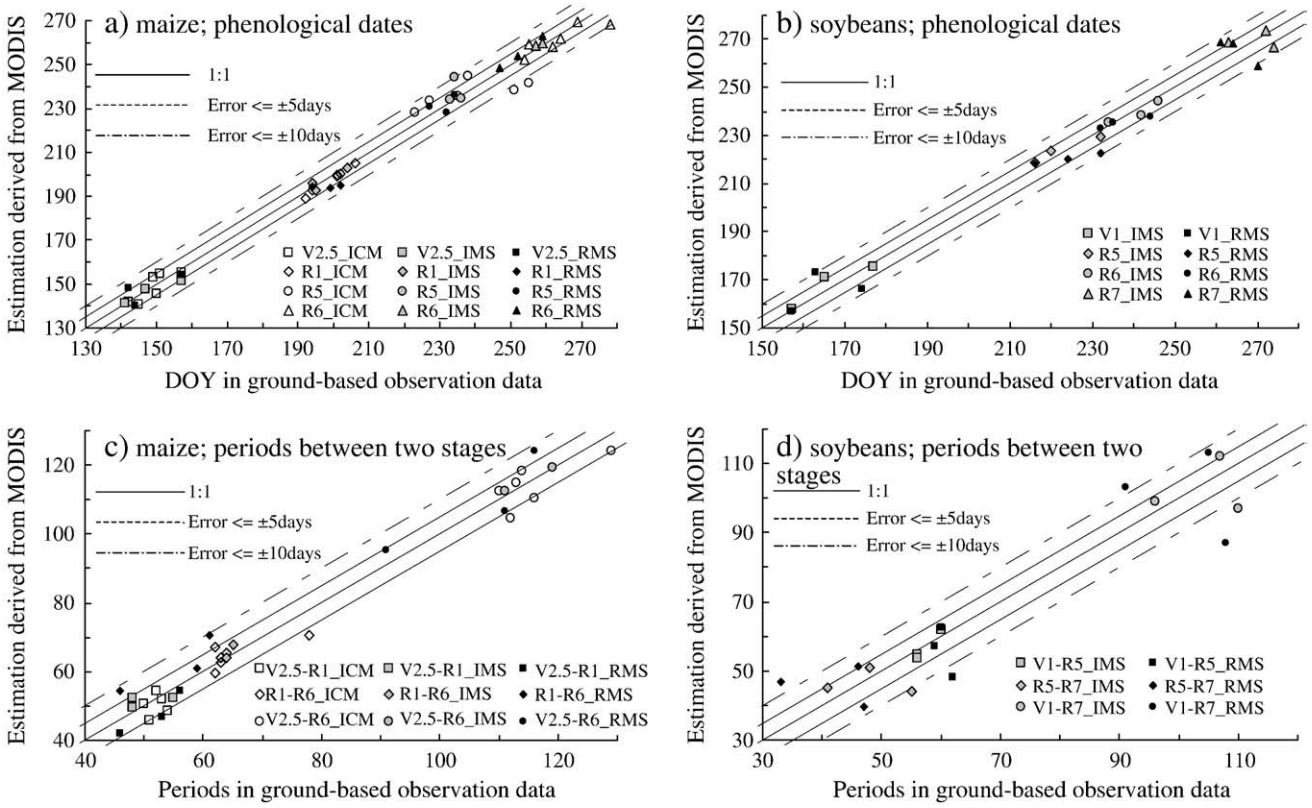

Fig. 5. Comparison of phenological dates (a: maize, b: soybean) and periods (c: maize, d: soybean) between ground-based observation data and MODIS-derived estimation.

conditions experienced over eastern Nebraska that year. The TSF method properly estimated the shorter growing season period in 2003 at the RMS site (V2.5 to R6 interval was 91 days observed on the ground and estimated to be 94.8 days) (Fig. 5b) compared to the other years, which ranged between 113 and 115 days in ground observations and TSF date estimates. This illustrates the potential of the TSF method when applied to MODIS 250-m data to provide relatively accurate estimate of the growing season length for maize (i.e., within 4–5 days of observed phenological date) and detect events such as the shortening of the growing season during a severe drought year. It also suggests that drought-affected maize areas might be identified based on growing season length recorded in the multi-temporal WDRVI, as well as the index's amplitude.

Although it is difficult to establish a statistically significant difference in estimation accuracy between the irrigated and rainfed study sites based on the limited number of validation data (maize at the RMS site: $n=3$, soybean at the RMS site: $n=3$), the RMSE of the estimated phenological date and growing season lengths of maize and soybean at the RMS site tended to be higher than those at the ICM or IMS sites with the exception of maize at the R5 stage (Tables 5 and 6). The scaling parameters (*xscale*, *yscale* and *tshift*) at the RMS site exhibited more variability across the study years than those of the ICM and IMS sites (Table 3), which illustrate the increased sensitivity of vegetation growth in the rainfed site to year-to-year fluctuations in precipitation patterns that are reflected by increased inter-annual variability in seasonal WDRVI curves at the RMS site. Therefore, the imperfect fitting of the shape model to the smoothed WDRVI data at the rainfed site resulted in a slightly lower accuracy of phenology date estimation as compared to results of the irrigated sites. However, the date differences between the irrigated and non-irrigated sites for most phenological stages were minimal (i.e., ~1 to 4 day difference).

8.2. Comparison of estimation accuracy between the TSF method and the two simple methods for the maize R1 and soybean R5 stages

The summary of the estimation accuracy of the maize R1 and soybean R5 stages using the three different methods (TSF, ORG and WBF) is shown in Table 7 and a comparison of those dates with the ground-based crop growth observations is shown in Fig. 6.

The RMSE of TSF-derived maize R1 dates (RMSE: 2.4 days) across all three sites (ICM + IMS + RMS, $n=12$) was considerably lower than the ORG (8.8 days) and WBF (8.5 days) RMSEs. The dates calculated with the TSF method were ~6 days closer to the observed maize R1 stage than those provided by the two simple methods. In addition, the TSF method had a fewer number of cases 1 (or 8% of the total cases) in which the date estimation error exceeded ±5 days compared to the ORG and WBF methods that had 4 (or 33%) and 6 (or 50%) cases, respectively. The TSF method provided consistently more accurate estimates of maize R1 stages than both ORG and WBF approaches.

Table 7
Accuracy comparison when the phenological dates R1 of maize and R5 of soybean are estimated by the three different methods (ORG, WBF and TSF).

Crop	Management	RMSE (days) [R]			n[a]
		ORG	WBF	TSF	
Maize	ICM	10.4 [−0.48]	7.3 [0.39]	0.7 [0.99]	6[b]
	IMS	5.2 [–]	5.5[–]	2.4 [–]	3
	RMS	8.1 [–]	12.4 [–]	4.1 [–]	3
	IMS + RMS	6.8 [0.42]	9.6 [0.53]	3.4 [0.59]	6
	ICM + IMS + RMS	8.8 [0.00]	8.5 [0.46]	2.4 [0.84]	12[b]
Soybean	IMS	4.5 [–]	5.2 [–]	4.2 [–]	3[c]
	RMS	5.8 [–]	4.8 [–]	5.8 [–]	3
	IMS + RMS	5.2 [0.78]	5.0 [0.96]	5.1 [0.68]	6[c]

[a] n is number of comparison data.
[b] Includes the 6 pixels used for making the shape model (ICM 2003–2008).
[c] Includes the 2 pixels used for making the shape model (IMS 2004, 2008).

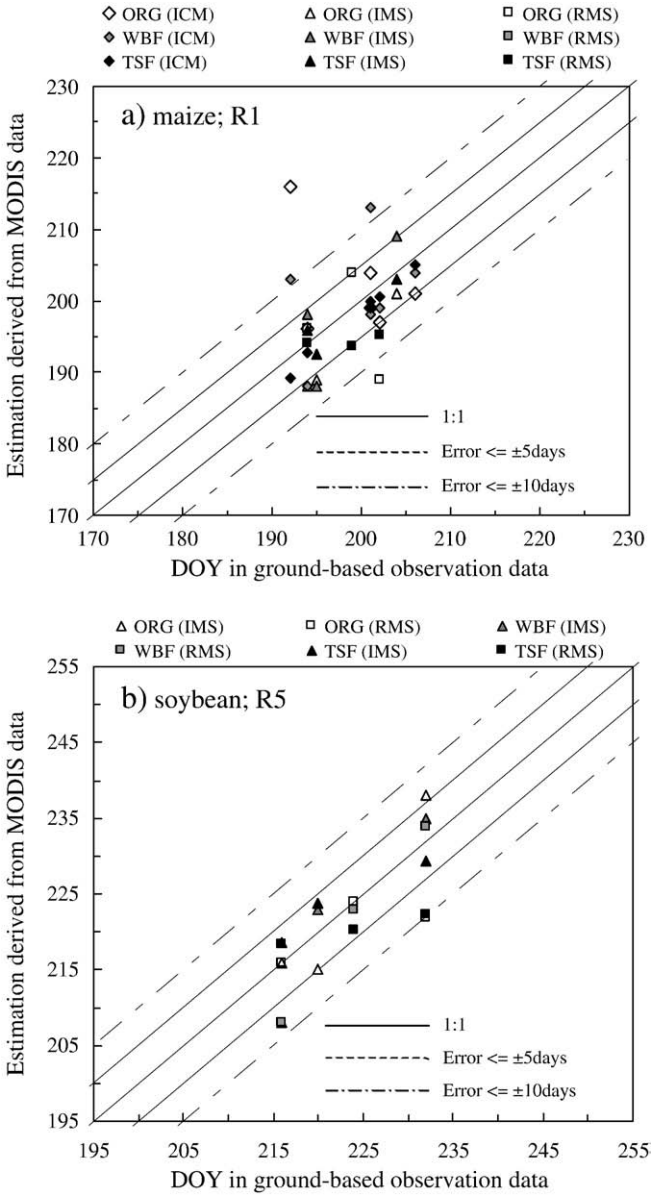

Fig. 6. One-to-one comparison between the ground-based observation data and the phenological dates, R1 of maize (a) and R5 of soybean (b), which are estimated by using the original time-series WDRVI data (ORG), the smoothed data using wavelet-based filter (WBF) and the two-steps filter (TSF).

On the other hand, the predictive accuracy of the TSF method for estimating the soybean R5 date was found to be similar to the other two methods. The RMSE of the soybean R5 date estimation was almost the same for the three methods (~5 days difference from the observed date), but the correlation coefficient of the WBF ($R=0.96$) was higher than that of the TSF ($R=0.68$). The similarity of the results among these three methods for soybean as compared to maize may be linked to shape differences in the two crop's WDRVI curves. The shape of maize WDRVI curve is like a quadrangle with left–right asymmetry, whereas the soybean WDRVI curve has a relatively uni-modal, symmetrical shape. Then, we speculated that the less complex WDRVI behavior exhibited by soybean may not activate the effects of the TSF method for improving estimates of dates such as soybean R5 stage. The higher correlation of the WBF for soybean may be partially due to this simpler geometry of seasonal soybean WDRVI curve (Fig. 3). The WBF method, which uses a wavelet-based filter with the mother wavelet (coiflet, order = 4), is functional enough to reconstruct the maximum point of the simple uni-modal shape

expressed in the soybean WDRVI time series that is similar to that rice phenology observed by Sakamoto et al. (2005). Although the TSF concept, which utilizes shape-model fitting, may not yield improved date estimates for crops that have a symmetrical, uni-modal WDRVI curve like soybean, the results from this comparison suggest that the shape-model fitting procedure would be effective for more complex WDRVI profiles with many vertices like maize.

Fig. 7 presents an example of a rescaled shape model for the RMS site in 2005 with the maize R1 date estimates from the TSF, ORG and WBF methods. The estimated maize R1 dates for the ORG (DOY: 204) and WBF (DOY: 218) methods were later than the observed date (DOY: 199). In contrast, the TSF method could estimated the maize R1 date (DOY: 196.0) slightly earlier than the site observation. The influence of non-vegetation-related noise in the original MODIS-based WDRVI time series is illustrated in the ORG curve in a sharp decrease in WDRVI values near DOY 205, which resulted in a later appearance of the maximum WDRVI point and later R1 date estimate compared to the ground observation. In the WDRVI time-series used for the WBF run in which, this noise was minimized using a wavelet-based filter, a much later R1 date was estimated because the wavelet-based filter rounded off the local part of WDRVI profile around the R1 stage and caused the later appearance of the maximum WDRVI. This illustrates the influence of that subtle, non-vegetation-related change in the temporal WDRVI profile can have on date estimates using the ORG and WBF methods. In comparison, the TSF method searches the optimum scaling parameters that geometrically fit a preliminary defined shape model on the observed WDRVI data and can estimate specific phenological dates by the computational expression of these parameters without being directly influenced by noise-related anomalies like the downward spike shown in original WDRVI time series in Fig. 7. In this example, the TSF method was the least influenced by this anomalous feature and estimated the R1 date within 3 days of the observed date. This example illustrates the TSF method's robustness to such non-vegetation-related variations that are often encountered in time-series VI data, which can lead to larger errors in phenological date estimates using more traditional phenology detection methods.

Conventional methods such as the ORG and WBF also have to apply the different metrics (e.g., maximum and inflection points) for estimating individual phenological events such as the green up (e.g., maize V2.5 and soybean V1) and maturity (e.g., maize R6 and soybean R7) stages. When different methods are required to estimate the full suite of targeted phenological stages, there is a possibility that the estimation error for a phenological event such as growing season length can be amplified by two kinds of errors. For growing season length, estimation errors can occur for two separate metrics that are typically used to identify the start (green up) and end (maturity) of the growing season. In contrast, the TSF method does not focus on the localized features in time-series WDRVI data around the green up and maturity stages but rather derives optimum scaling parameters (*xscale* and *tshift*) representing the macroscopic features in time-series WDRVI data. Multiple phenological dates are then estimated at the same time through a geometric conversion equation (Eq. (4)) using the common scaling parameters (*xscale* and *tshift*) to avoid the influence of the localized fluctuations in the time-series WDRVI data. Furthermore, the TSF method may have applicability to other crops such as sorghum, sugar cane, and winter wheat, which have well-defined crop calendars that can be used to define key phenological stages and guide the development of a shape model for the crop.

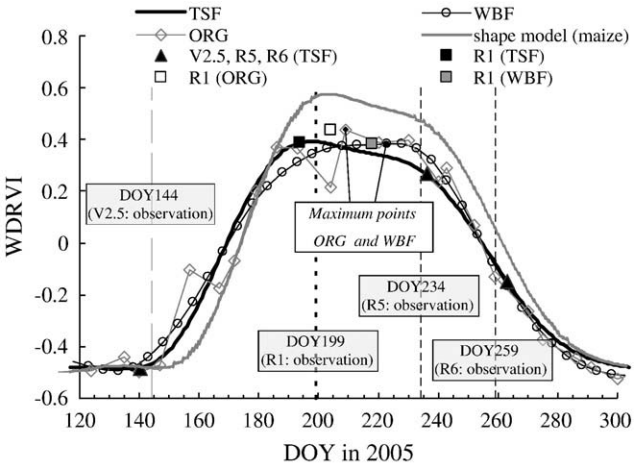

Fig. 7. The difference in the estimated R1 date between the three methods (ORG, WBF and TSF) for data from maize of RMS 2005.

8.3. Region-based verification in eastern Nebraska from 2001 to 2002

Fig. 8 shows the comparison of the ASD-level median dates of key developmental stages between the TSF method and the NASS-CPR from 2001 to 2002. The median, ASD-level date estimates for the key

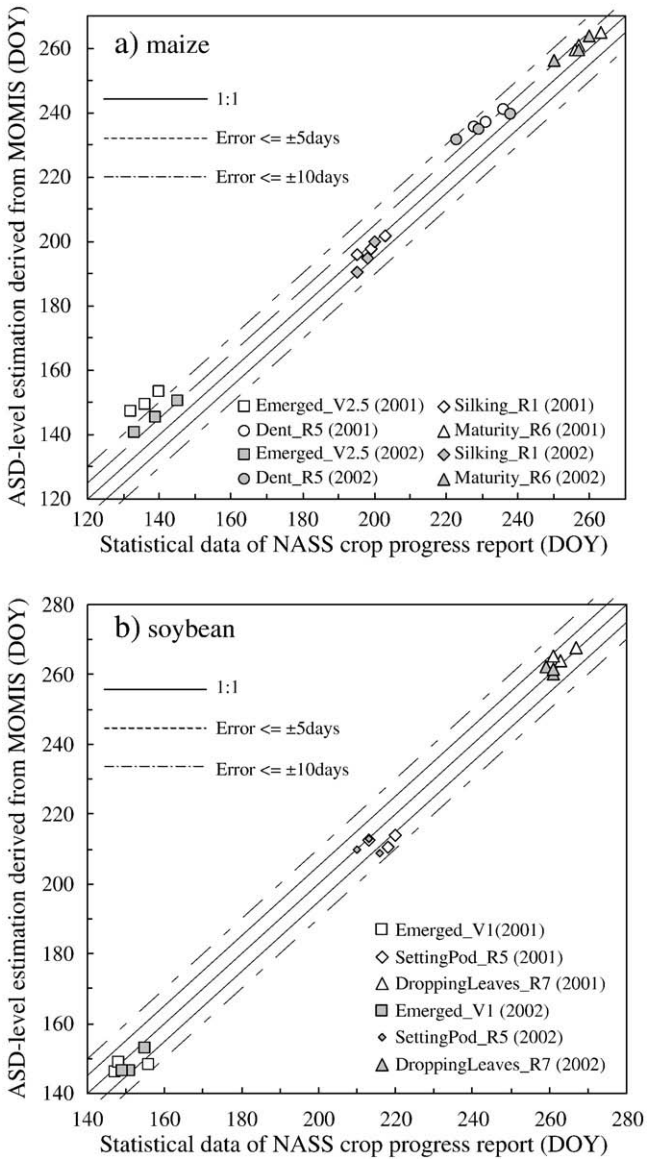

Fig. 8. Comparison of phenological dates (a: maize, b: soybean) between statistical data of NASS crop progress reports and MODIS-derived estimation in three Agricultural Statistics Districts (ASD) on eastern Nebraska from 2001 to 2002.

phenological dates targeted for maize (V2.5 RMSE: 4.1 days [with bias correction of 10 days] $R=0.59$; R1 RMSE: 1.6 days $R=0.88$; R5 RMSE: 5.6 days $R=0.96$; R6 RMSE: 3.3 days $R=0.96$) and soybean (V1 RMSE: 4.1 days $R=0.63$; R5 RMSE: 5.3 days $R=0.30$; R7 RMSE: 2.5 days $R=0.78$) were in good agreement with the NASS reported crop progress dates for all three districts tested in eastern Nebraska. Overall, the date difference between the estimated and observed dates was less than 9 days for all phenological stages with the exception of the emerged/V2.5 date of maize. However, some temporal difference between the emergence date in the NASS

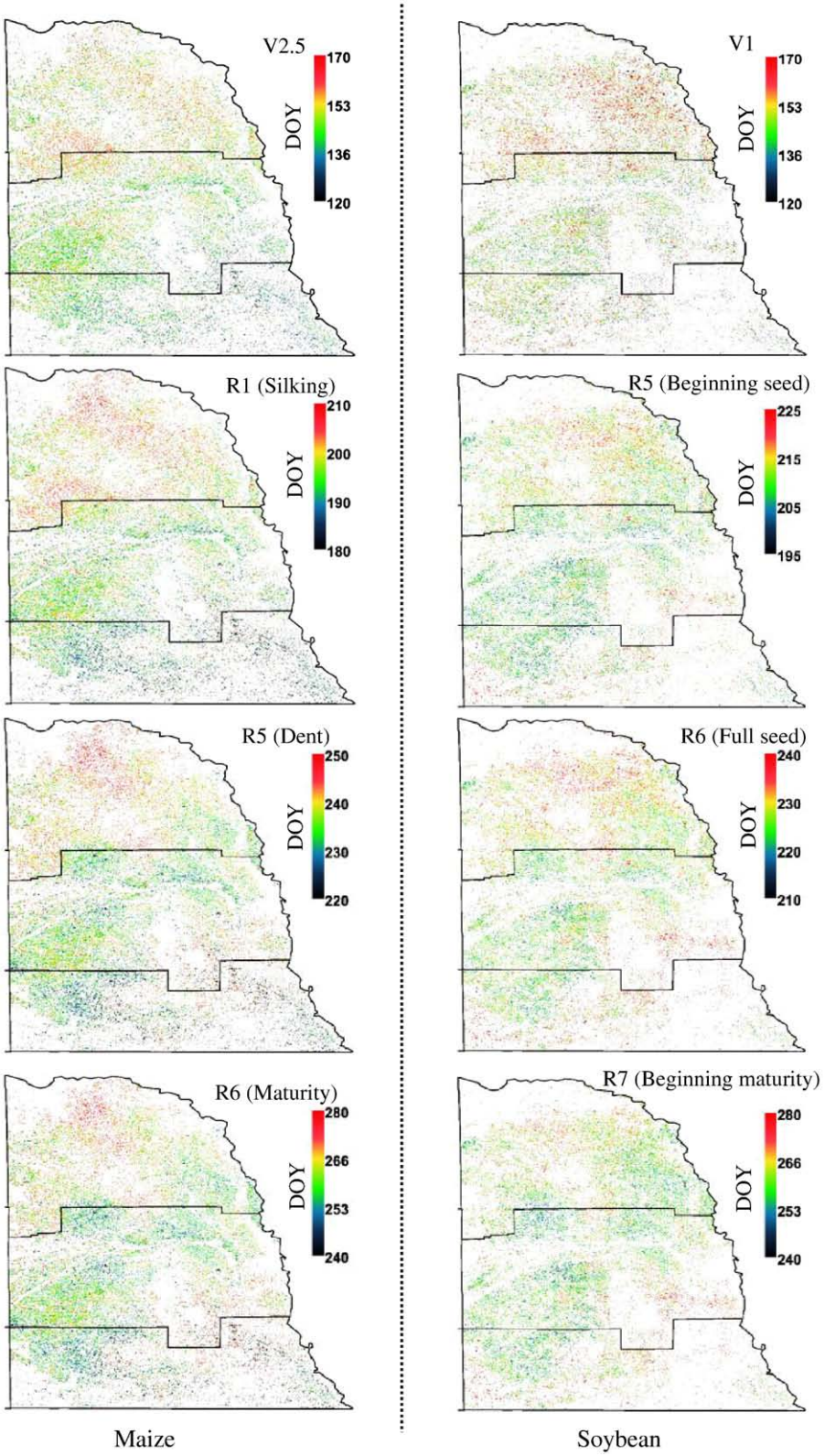

Fig. 9. Spatial patterns of the date of key crop developmental stages in eastern Nebraska, 2002. The Two-Step Filtering method was applied to the pixels which the area ratio of target crops (maize or soybean) is over 75% in basis of the NASS-Crop Data Layer.

statistics and the estimated agronomic stage date would be expected because they are representing slightly different events. In the case of emergence, NASS is reporting when plants have broken the soil's surface, whereas the V2.5 stage for maize represents early-stage, post-emergence leaf development. As a result, some lag between the NASS date and MODIS-based date estimate using the TSF method would be expected for this early growth stage. For example, Hicks et al. (1999) indicated that approximately 4 days are required for maize to leaf out during the early vegetative stages. As a result, the dates of the early vegetative growth stage, as well as the other targeted phenological stage dates estimated with the TSF method from MODIS 250-m WDRVI were within a week or less of the equivalent crop stage reported by NASS for all three ASDS in 2001 and 2002. The ASD-level results illustrate that the MODIS-based TSF approach can be extended over a larger geographic area and maintain a similar level of date estimation accuracy as was observed over the three local-scale study sites.

Fig. 9 shows spatial distributions of MODIS-derived phenological stages of maize and soybean across the three ASDs in eastern Nebraska for 2002. In general, the north–south planting date gradient that occurs across eastern Nebraska is represented in the series of phenology stage maps with the earliest V2.5 dates occurring in the southeast district (blue areas) and the latest occurring in the northeast district (red areas). In general, the start of maize planting occurs when the average daily air temperature exceeds 55 °F and then soil temperature is enough warm to initiate germination (Neild, 1981; Neild & Newman, 1986). Soybean planting also begins when the soil temperature is warmer enough for the seeds to germinate (Elmore & Flowerday 1984). On average, southeast Nebraska has a longer growing season of 160 freeze-free days (3100 growing degree days) and earlier planting dates (Neild, 1986), which are reflect by the early dates estimates for each phenological stage of maize in Fig. 9. In contrast, northeast Nebraska has a shorter growing season of 130 freeze-free days (2200 growing degree days) and later planting dates (Neild, 1986), which are represented by the later date estimates for each phenological stage. However on closer inspection of the maps, there is the difference in relative north–south time range of the MODIS-derived estimates between maize and soybean. The north–south gradient of the estimated phenological dates of soybean is subtler than for maize with a narrow date range difference between the north and the south (Figs. 8 and 9). There is the major difference between maize and soybean in terms of their physiological response to seasonal environmental changes. Comparing the succession of developmental stages of maize is closely related to accumulated air temperature, the shift from the vegetative to the flowering stage in soybean is more closely related to photoperiod (day length effect) (Elmore & Flowerday, 1984). Thus, the difference in the environmental response between the thermosensitive crop (maize) and the photosensitive crop (soybean) might characterize the time range of the MODIS-derived phenology map. It should also be noted that the local-scale variations within each ASD for each of the four maize and soybean phenology date maps generated from the MODIS 250-m data, which illustrates the value of using this type of remote sensing-based crop phenology estimation approach to monitor their local-scale spatio-temporal variations. The results of region-based verification confirmed that the MODIS-derived estimations using the TSF method could evaluate the spatio-temporal patterns of maize and soybean phenology with reasonable estimation accuracy.

9. Conclusions

In this study, we proposed a new approach named the Two-Step Filtering method (TSF) for detecting the specific phenological dates of maize (V2.5, R1, R5 and R6) and soybean (V1, R5, R6 and R7) from time-series MODIS 250-m data. A novel shape-model fitting concept was incorporated into the TSF approach. The advantage of the TSF method is that the estimation results are less affected by the subtle, localized fluctuations in the WDRVI profile compared to more common methods that focus on the local-scale changes (e.g. maximum VI point) in the VI profile in their estimates.

We applied the TSF method to MODIS-derived WDRVI data over a 6-year period (2003 to 2008) for two irrigated sites and one rainfed site planted to maize or soybean and evaluated the estimation accuracy of the MODIS-derived phenological dates by using ground-based crop growth stage observations collected for the same sites across the six study years. The target crop phenological stages of maize were V2.5 (early vegetative stage), R1 (silking), R5 (denting), and R6 (maturity). The stages for soybean were V1 (early vegetative stage), R5 (beginning seed), R6 (full seed), and R7 (beginning maturity). The pixel-based validation at the site level confirmed that the TSF method was able to estimate these four phenological stages of maize and soybean with reasonable accuracy that the RMSE for maize ranged from 2.4 [R1] to 7.4 [R5] days and from 3.0 [R6] to 7.0 [R7] days for soybean. The TSF method was also applied for three agricultural statistic districts in eastern Nebraska for 2001 to 2002 and the regional, MODIS-based date estimates results were found to have a high level of agreement with the crop phenology dates reported in the district-level NASS-CPR statistics. The ASD-level RMSE for maize ranged from 1.6 [R1] to 5.6 [R5] days and from 2.5 [R6] to 5.3 [R5] days for soybean, which was comparable to the site-level results. The TSF method presented in this paper proved to be a viable approach for the accurate estimation of key phenological dates of maize and soybean and also has been shown to be relatively robust in its calculations over multiple years.

Because of the limited number of ground-based observations in this study, further analysis with other ground-based observations about various cultivars planted at different geographic locations is needed to verify the general versatility of the TSF method. Future research is planned that will collect additional ground-based observational data and apply this method at a larger regional-scale across the U.S. Corn Belt in an effort to investigate the intra-annual spatio-temporal variations in maize and soybean phenology and assess their inter-annual changes over a multi-year study period. Operational crop phenology monitoring over large areas would lead to mapping spatio-temporal variations in various phenological characteristics, and result in a better assessment of intra-annual variations in crop conditions across key agricultural regions.

Acknowledgements

We gratefully acknowledge the use of facilities and equipment provided by the National Drought Mitigation Center (NDMC), University of Nebraska-Lincoln (UNL). We are grateful to Dr. Don ald A. Wilhite, Dr. Mike J. Hayes, Dr. Tsegaye Tadesse, Mr. Todd T. Schimelfenig, Ms. Deborah A. Wood and Mr. James R. Hines of SNR for their valuable comments and research support. We would thank three anonymous reviewers for their valuable comments and suggestions. This work was financially supported by the Japanese Society for the Promotion of Science; JSPS Postdoctoral Fellowships for Research Abroad.

References

Azzali, S., & Menenti, M. (2000). Mapping vegetation–soil–climate complexes in southern Africa using temporal Fourier analysis of NOAA-AVHRR NDVI data. *International Journal of Remote Sensing*, *21*, 973−996.

Badhwar, G. D. (1984). Automatic corn–soybean classification using Landsat MSS data. I — Near-harvest crop proportion estimation. II — Early season crop proportion estimation. *Remote Sensing of Environment*, *14*, 15−29.

Badhwar, G. D., Garnes, J. G., & Austin, W. W. (1982). Use of Landsat-derived temporal profiles for corn–soybean feature extraction and classification. *Remote Sensing of Environment*, *12*, 57−79.

Bauer, M. E. (1985). Spectral inputs to crop identification and condition assessment. *Proceedings of the IEEE*, *73*, 1071−1085.

Brown, J. C., Jepson, W. E., Kastens, J. H., Wardlow, B. D., Lomas, J. M., & Price, K. P. (2007). Multitemporal, moderate-spatial-resolution remote sensing of modern agricultural production and land modification in the Brazilian Amazon. *Giscience & Remote Sensing*, *44*, 117−148.

Chang, J., Hansen, M. C., Pittman, K., Carroll, M., & DiMiceli, C. (2007). Corn and soybean mapping in the united states using MODN time-series data sets. *Agronomy Journal*, *99*, 1654−1664.

Dale, R. F., Coelho, D. T., & Gallo, K. P. (1980). Prediction of daily green leaf area index for corn. *Agronomy Journal*, *72*, 999−1005.

de Beurs, K. M., & Henebry, G. M. (2004). Land surface phenology, climatic variation, and institutional change: Analyzing agricultural land cover change in Kazakhstan. *Remote Sensing of Environment*, *89*, 497−509.

Elmore, R. W., & Flowerday, A. D. (1984). G84-687 soybean planting date: When and why. *Historical Materials from University of Nebraska-Lincoln Extension* (pp. 736).

Funk, C., & Budde, M. E. (2009). Phenologically-tuned MODIS NDVI-based production anomaly estimates for Zimbabwe. *Remote Sensing of Environment*, *113*, 115−125.

Galford, G. L., Mustard, J. F., Melillo, J., Gendrin, A., Cerri, C. C., & Cerri, C. E. P. (2008). Wavelet analysis of MODIS time series to detect expansion and intensification of row-crop agriculture in Brazil. *Remote Sensing of Environment*, *112*, 576−587.

Gallo, K. P., & Flesch, T. K. (1989). Large-area crop monitoring with the NOAA AVHRR: Estimating the silking stage of corn development. *Remote Sensing of Environment*, *27*, 73−80.

Gitelson, A. A. (2004). Wide dynamic range vegetation index for remote quantification of biophysical characteristics of vegetation. *Journal of Plant Physiology*, *161*, 165−173.

Gitelson, A. A., Wardlow, B. D., Keydan, G. P., & Leavitt, B. (2007). An evaluation of MODIS 250-m data for green LAI estimation in crops. *Geophysical Research Letters*, *34*.

Henderson, K. E., & Badhwar, G. D. (1982). An initial model for estimating soybean development stages from spectral data. *Machine processing of remotely sensed data: Crop inventory and monitoring* (pp. 199−205).

Hicks, R. D., Naeve, L. S., & Bennett, M. J. (1999). The corn growers field guide for evaluating crop damage and replant options: University of Minnesota Printing Services. Available at:http://www.soybeans.umn.edu/pdfs/CornGuide.pdf

Hickman, J. S., & Shroyer, J. P. (1994). Corn production handbook. *Manhattan, Kansas: Publication C-560* (pp. 44). Manhattan, Kansas: Kansas State University Agricultural Experiment Station and Cooperative Extension Service.

Hill, M. J., & Donald, G. E. (2003). Estimating spatio-temporal patterns of agricultural productivity in fragmented landscapes using AVHRR NDVI time series. *Remote Sensing of Environment*, *84*, 367−384.

Islam, A. S., & Bala, S. K. (2008). Assessment of potato phenological characteristics using MODIS-derived NDVI and LAI information. *Giscience & Remote Sensing*, *45*, 454−470.

Jakubauskas, M. E., Legates, D. R., & Kastens, J. H. (2001). Harmonic analysis of time-series AVHRR NDVI data. *Photogrammetric Engineering and Remote Sensing*, *67*, 461−470.

Jakubauskas, M. E., Legates, D. R., & Kastens, J. H. (2002). *Crop identification using harmonic analysis of time-series AVHRR NDVI data* (pp. 127−139).

Kang, S. Y., Running, S. W., Lim, J. H., Zhao, M. S., Park, C. R., & Loehman, R. (2003). A regional phenology model for detecting onset of greenness in temperate mixed forests, Korea: An application of MODIS leaf area index. *Remote Sensing of Environment*, *86*, 232−242.

Kilgore, G. L., & Fjell, D. L. (1997). *Soybean production handbook* (pp. 32).

Lasdon, L. S., Waren, A. D., Jain, A., & Ratner, M. (1978). Design and testing of a generalized reduced gradient code for nonlinear programming. *ACM Transactions on Mathematical Software (TOMS)*, *4*, 34−50.

Loveland, T. R., Merchant, J. W., Brown, J. F., Ohlen, D. O., Reed, B. C., Olson, P., et al. (1995). Seasonal land-cover regions of the United States. *Annals of the Association of American Geographers*, *85*, 339−355.

Loveland, T. R., Reed, B. C., Brown, J. F., Ohlen, D. O., Zhu, Z., Yang, L., et al. (2000). Development of a global land cover characteristics database and IGBP DISCover from 1 km AVHRR data. *International Journal of Remote Sensing*, *21*, 1303−1330.

NASS (2010). National Agricultural Statistics Service (NASS). In.

Neild, R. E. (1981). G81-552 effects of weather on corn planting and seedling establishment. *Historical Materials from University of Nebraska-Lincoln Extension* (pp. 750).

Neild, R. E. (1986). G86-796 growing degree day requirements and freeze risk as a guide to selecting and planting corn hybrids. *Historical Materials from University of Nebraska-Lincoln Extension* (pp. 720).

Neild, R. E., & Newman, J. E. (1986). Growing season characteristics and requirements in the Corn Belt. *National corn handbook NCH-40*. West Lafeyette, IN: Purdue University.

Ozdogan, M., & Gutman, G. (2008). A new methodology to map irrigated areas using multi-temporal MODIS and ancillary data: An application example in the continental US. *Remote Sensing of Environment*, *112*, 3520−3537.

Reed, B. C., Brown, J. F., Vanderzee, D., Loveland, T. R., Merchant, J. W., & Ohlen, D. O. (1994). Measuring phenological variability from satellite imagery. *Journal of Vegetation Science*, *5*, 703−714.

Reed, B. C., Loveland, T. R., & Tieszen, L. L. (1996). An approach for using AVHRR data to monitor US Great Plains grasslands. *Geocarto International*, *11*, 13−22.

Sakamoto, T., Phung, V. C., Nhan, V. N., Kotera, A., & Yokozawa, M. (2009). Agro-ecological interpretation of rice cropping systems in flood-prone areas using MODIS imagery. *Photogrammetric Engineering and Remote Sensing*, *75*, 413−424.

Sakamoto, T., Van Nguyen, N., Kotera, A., Ohno, H., Ishitsuka, N., & Yokozawa, M. (2007). Detecting temporal changes in the extent of annual flooding within the Cambodia and the Vietnamese Mekong Delta from MODIS time-series imagery. *Remote Sensing of Environment*, *109*, 295−313.

Sakamoto, T., Van Nguyen, N., Ohno, H., Ishitsuka, N., & Yokozawa, M. (2006). Spatio-temporal distribution of rice phenology and cropping systems in the Mekong Delta with special reference to the seasonal water flow of the Mekong and Bassac rivers. *Remote Sensing of Environment*, *100*, 1−16.

Sakamoto, T., Van, P., Kotera, A., Duy, K. N., & Yokozawa, M. (2009). Detection of yearly change in farming systems in the Vietnamese Mekong Delta from MODIS time-series imagery. *JARQ*, *43*, 173−185.

Sakamoto, T., Van Phung, C., Kotera, A., Nguyen, K. D., & Yokozawa, M. (2009). Analysis of rapid expansion of inland aquaculture and triple rice-cropping areas in a coastal area of the Vietnamese Mekong Delta using MODIS time-series imagery. *Landscape and Urban Planning*, *92*, 34−46.

Sakamoto, T., Yokozawa, M., Toritani, H., Shibayama, M., Ishitsuka, N., & Ohno, H. (2005). A crop phenology detection method using time-series MODIS data. *Remote Sensing of Environment*, *96*, 366−374.

Suyker, A. E., & Verma, S. B. (2009). Evapotranspiration of irrigated and rainfed maize–soybean cropping systems. *Agricultural and Forest Meteorology*, *149*, 443−452.

Townshend, J. R. G., & Justice, C. O. (1988). *Selecting the spatial resolution of satellite sensors required for global monitoring of land transformations*, *9*. (pp. 187−236).

Turner II, B. L., Skole, D. L., Sanderson, S., Fischer, G., Fresco, L., & Leemans, R. (1995). Land-use and land-cover change. Science/Research Plan. *Stockholm and Geneva: IGBP Report No. 35 and HDP Report No. 7* (pp. 132).

Vermote, E. F., El Saleous, N. Z., & Justice, C. O. (2002). Atmospheric correction of MODIS data in the visible to middle infrared: First results. *Remote Sensing of Environment*, *83*, 97−111.

Viovy, N., Arino, O., & Belward, A. (1992). The best index slope extraction (BISE) — a method for reducing noise in NDVI time-series. *International Journal of Remote Sensing*, *13*, 1585−1590.

Wardlow, B. D., & Egbert, S. L. (2008). Large-area crop mapping using time-series MODIS 250 m NDVI data: An assessment for the US Central Great Plains. *Remote Sensing of Environment*, *112*, 1096−1116.

Wardlow, B. D., Egbert, S. L., & Kastens, J. H. (2007). Analysis of time-series MODIS 250 m vegetation index data for crop classification in the US Central Great Plains. *Remote Sensing of Environment*, *108*, 290−310.

Wardlow, B. D., Kastens, J. H., & Egbert, S. L. (2006). Using USDA crop progress data for the evaluation of greenup onset date calculated from MODIS 250-meter data. *Photogrammetric Engineering and Remote Sensing*, *72*, 1225−1234.

White, M. A., Thornton, P. E., & Running, S. W. (1997). A continental phenology model for monitoring vegetation responses to interannual climatic variability. *Global Biogeochemical Cycles*, *11*, 217−234.

Xavier, A. C., Rudorff, B. F. T., Shimabukuro, Y. E., Berka, L. M. S., & Moreira, M. A. (2006). Multi-temporal analysis of MODIS data to classify sugarcane crop. *International Journal of Remote Sensing*, *27*, 755−768.

Xiao, X., Boles, S., Frolking, S., Salas, W., Moore, B., Li, C., et al. (2002). Observation of flooding and rice transplanting of paddy rice fields at the site to landscape scales in China using VEGETATION sensor data. *International Journal of Remote Sensing*, *23*, 3009−3022.

Zhang, X. Y., Friedl, M. A., Schaaf, C. B., Strahler, A. H., Hodges, J. C. F., Gao, F., et al. (2003). Monitoring vegetation phenology using MODIS. *Remote Sensing of Environment*, *84*, 471−475.